Electronic Supplementary Material (ESI) for Catalysis Science & Technology.

Electronic Supplementary Information for

Efficient and stable photocatalytic NO removal on C self-doped g-C_3N_4: electronic structure and reaction mechanism

Maoxi Ran [a], Jiarui Li [a], Wen Cui [a], Yuhan Li [a], Peidong Li [a], Fan Dong [a, *]

[a] Chongqing Key Laboratory of Catalysis and New Environmental Materials, College of Environment and Resources, Chongqing Technology and Business University, Chongqing 400067, China.

[*] To whom correspondence should be addressed. E-mail: dfctbu@126.com (Fan Dong). Phone: +86 23 62769785 605. Fax: +86 23 62769785 605.

Table of Context

Experimental section:

Characterization of photocatalysts

The crystal phases of the samples were analyzed by X-ray diffraction (XRD) with Cu Kα radiation (Model D/max RA Rigaku Co., Japan). Carton to nitrogen ration (C/N) of the samples was detected by elemental analysis (EA, Vario ELIII CHASO). The morphology and structure of the prepared photocatalysts were analyzed using scanning electron microscope (SEM, JEOL model JSM-6490, Japan), transmission electron microscope (TEM, JEM-2010, Japan). A nitrogen adsorption apparatus (ASAP 2010, USA) was used to detect the Brunauer-Emmett-Teller (BET) specific surface area (S_{BET}) of the obtained products with all samples degassed at 300 ℃ for 2 h prior to measurements. X-ray photoelectron spectroscopy (XPS) with Al Kα X-ray radiation (hv=1486.6 eV) operated at 150 W (Thermo ESCA-LAB 250, USA) was used to investigated the surface chemical compositions and states. Electron spin resonance (ESR) of radicals spin-trapped by 5,5-dimethyl-1-pyrroline noxide (DMPO) was recorded on a JES FA200 spectrometer. Samples for measurement were prepared by mixing the samples in 50 mM DMPO solution tanks (aqueous dispersion for DMPO-·OH and methanol dispersion for DMPO-$\cdot O_2^-$) and irradiated with visible light. Electron paramagnetic resonance (EPR) measurements were carried out on a Bruker ESP 500 spectrometer. Steady and time-resolved fluorescence emission spectra were recorded at room temperature with a fluorescence spectrophotometer (Ediburgh Instruments, ELSP-920). Photoluminescence (PL) studies (F-7000, HITACHI, Japan) and UV-vis diffuse reflectance spectra (UV-vis DRS) were obtained for the dry-pressed disk samples using a scanning UV-vis spectrophotometer (UV-vis DRS, UV-2450, Shimadzu, Japan) equipped with an integrating sphere assembly to investigate the optical properties of the samples.

Evaluation of photocatalytic activity

The photocatalytic activity was evaluated by the removal efficiency of NO at ppb levels in a continuous flow reactor at ambient temperature. The rectangular reactor (30 cm × 15 cm × 10 cm) is made of polymeric glass and covered with Saint-Glass. A

150 W commercial tungsten halogen lamp (the average light intensity was 0.16 W/cm^2) was vertically placed outside and 20 cm above the reactor. The UV light in the light beam was removed by adopting a UV cutoff filter (420 nm). The as-prepared sample (0.20 g) was dispersed in absolute ethyl alcohol (25 mL) via ultrasonic treatment. The resulting suspension was coated onto two glass dishes (12.00 cm in diameter) and then pretreated at 55 °C to remove ethyl alcohol. The NO gas acquired from a compressed gas cylinder at a concentration of 100 ppm of NO (N_2 balance). The initial concentration of NO was diluted to about 550 ppb by a zero air generator. And the relative humidity (RH) level of the NO flow was controlled at 50% by passing the air stream through a humidification chamber. The flow rates of the air stream and NO were controlled at 2.4 L/min and 15 mL/min, respectively. The lamp was turned on when the adsorption-desorption equilibrium was achieved. The concentration of NO was continuously measured by a NO_X analyzer (Thermo Environmental Instruments Inc., model 42c-TL), which can monitor the concentration of NO, NO_2 and NO_X (NO_X represents NO + NO_2). The removal ratio (η) of NO was calculated as $\eta = (1 - C/C_0) \times 100\%$, where C and C_0 are the concentrations of NO in the outlet steam and the feeding stream, respectively.

Scheme:

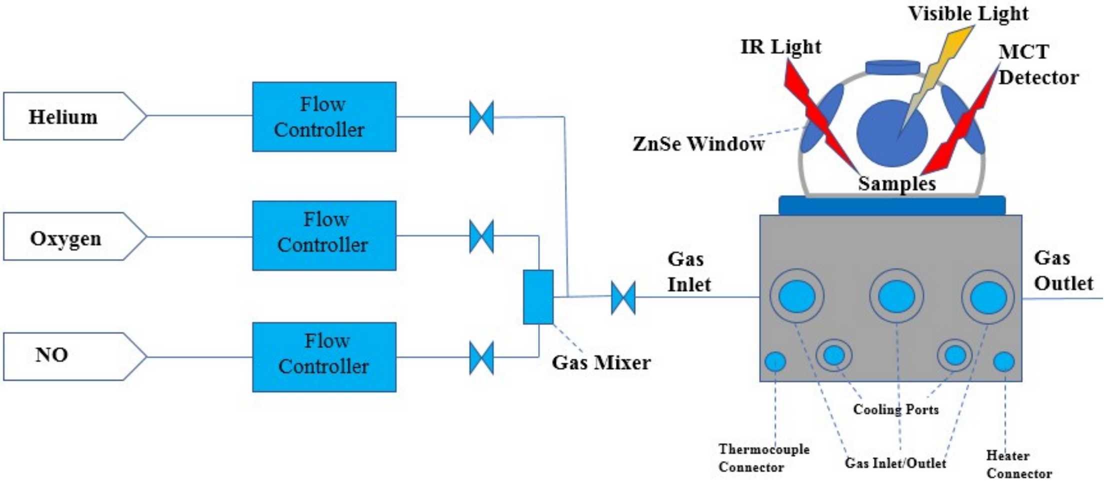

Scheme S1 The designed reaction system for the *in situ* DRIFTS signal recording.

Figures:

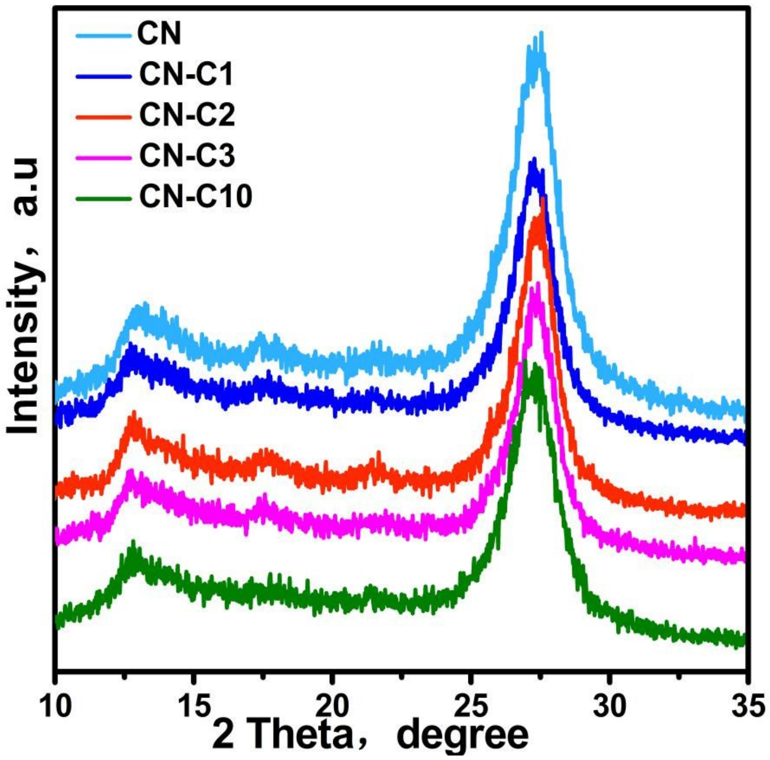

Fig. S1 XRD patterns of all as-prepared samples.

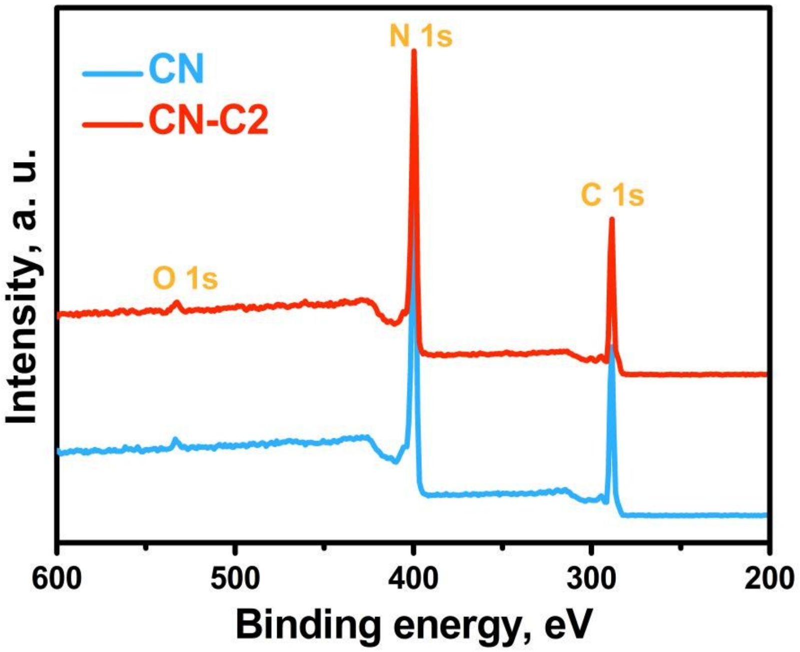

Fig. S2 The survey spectra of CN and CN-C2.

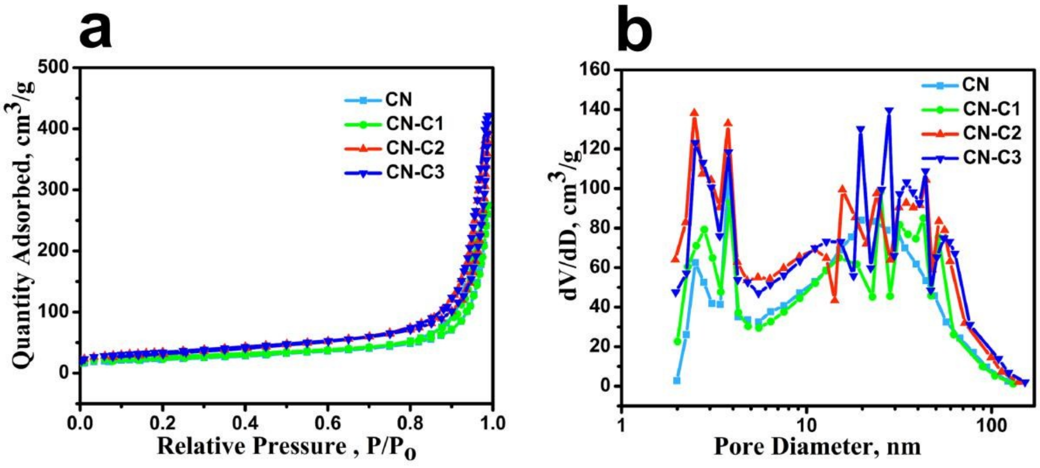

Fig. S3 N2 adsorption-desorption isotherms curves (a) and pore-size distribution (b) of as-prepared samples.

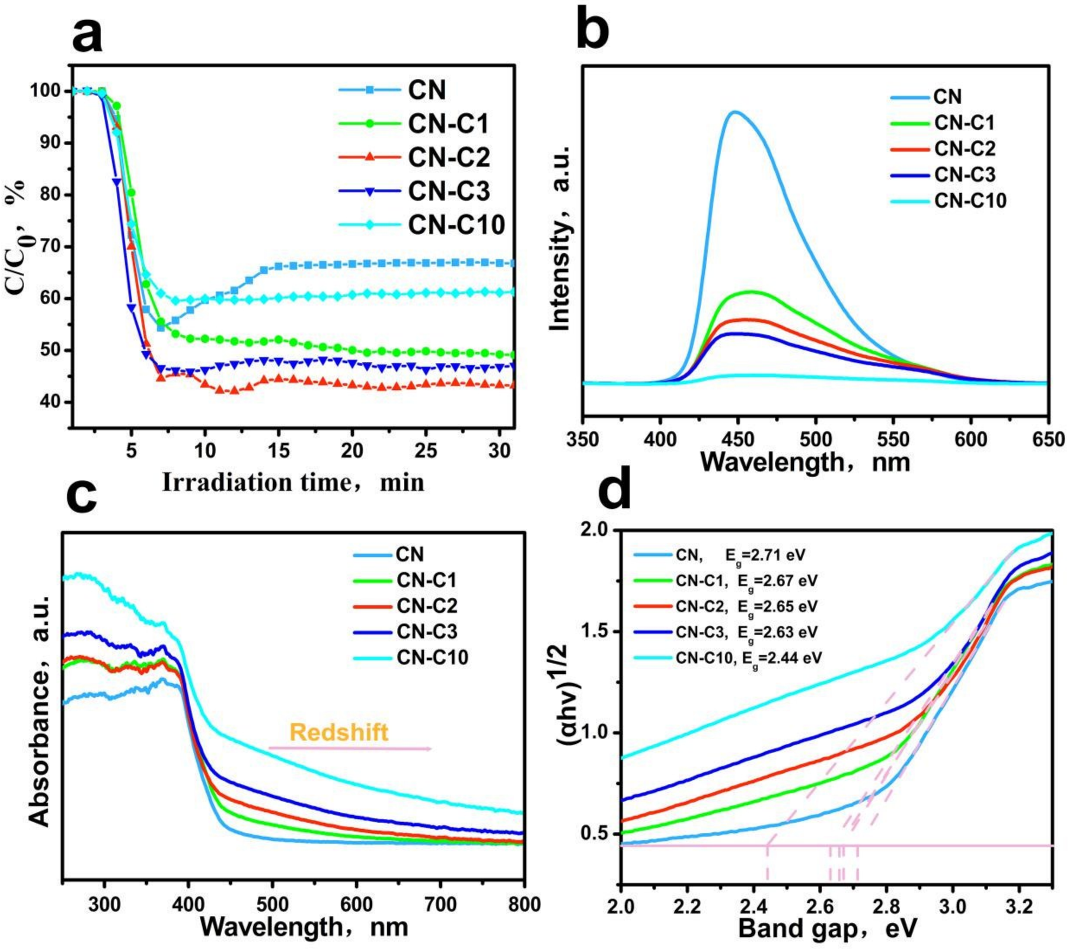

Fig. S4 Photocatalytic activity of all the as-prepared samples towards NO removal (a); photoluminescence spectra of the as-obtained samples (b); The UV-vis spectra of all as-prepared samples (c); the estimated band gaps of the as-obtained samples (d).

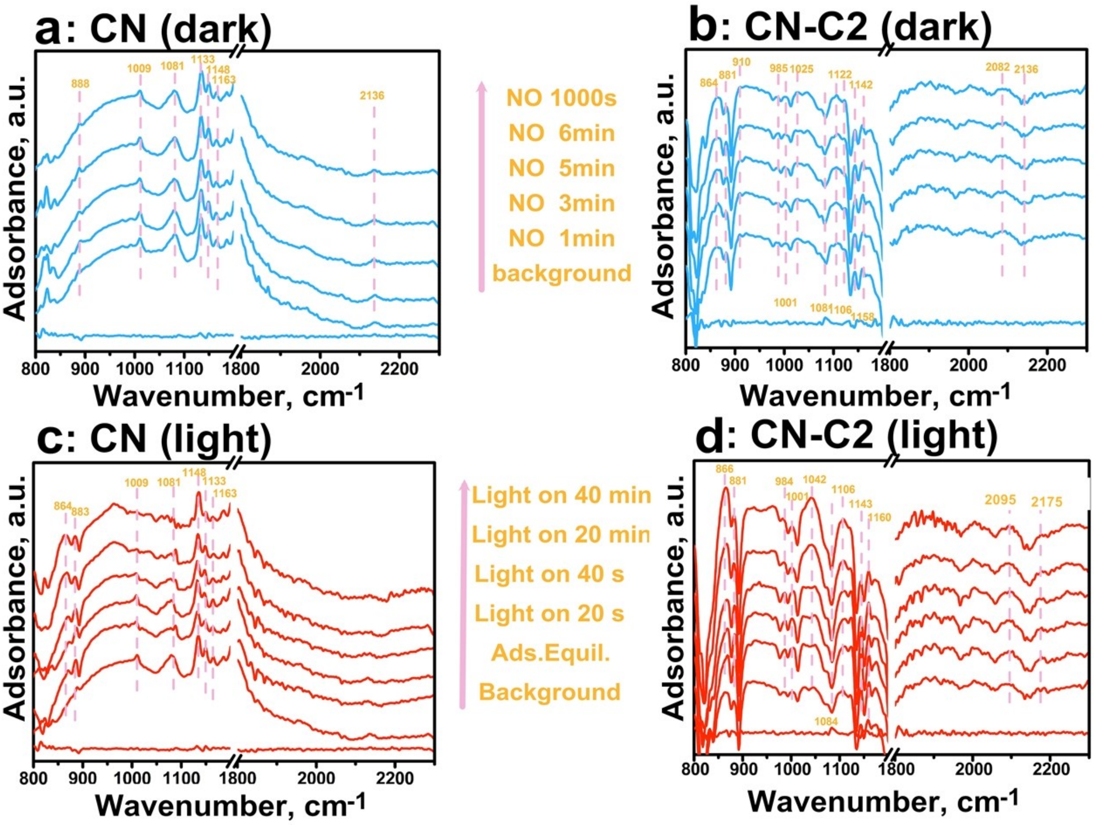

Fig. S5 In situ IR spectra of NO adsorption and visible light reaction processes over CN and CN-C.

To reveal reaction mechanism of photocatalytic NO oxidation over CN and CN-C2, in situ DRIFTS was employed to monitor the reaction intermediates and final products on the surface of as-prepared photocatalysts in chronological order, as shown in Fig 7. The background spectrum was recorded before injecting NO into the reaction chamber. NO adsorption bands appear under dark conditions when NO contact with the photocatalyst. As shown in Fig.S5a, the adsorption bands of N_2O (2136 cm^{-1}) and NO^-/NOH (1133, 1148 and 1163 cm^{-1}) can be observed.[1, 2, 3] Additionally, the other adsorption bands center at 888, 1009 and 1081 cm^{-1} (Fig. S5a) can be assigned to NO^{2-}, nitrates and bidentate nitrates or monodentate nitrites, respectively.[4, 5, 6, 7, 8] With the progress of adsorption reaction, the intensity of absorption bands locate at 888, 1081 cm^{-1} (Fig. S5a) were increased progressively, indicating the gradual accumulation of nitrites and nitrates compounds and the chemical adsorption of NO on the surface of CN. The formation of nitrates and nitrites ascribed to the active two-coordinated N atoms, which promote the formation of the activated oxygen species that could boost the oxidation ability of surface oxygen species for NO oxidation.[9, 10] After adsorption equilibrium reached, the time-dependent IR spectra of CN under visible light irradiation were recorded dynamically. As shown in Fig. S5c, the absorbance band centered at 2136 cm^{-1} disappears, the intensity of adsorption bands at 883, 1081 cm^{-1} becomes more obvious, which indicated that there are more NO can be converted to nitrites and nitrates. What's more, new absorption band locates at 864 cm^{-1} (Fig. S5c) was detected, which can be attributed to the final products of photocatalytic NO oxidation (chelated nitrite).[11] Table S2-S5 summaries the assignment of adsorption bands for CN and CN-C2 samples.

Compared with CN (Fig. S5b), new absorption bands of CN-C2 were detected at 910 cm^{-1} , 1025 cm^{-1} , 2095 cm^{-1} (N_2O_4, NO, NO_2), indicating more intermediate products were generated. Meanwhile, there are more adsorption band at 985 cm^{-1} (chelating bidentate NO^{3-} species), 1106 cm^{-1} (nitrites), 1122 cm^{-1} (bidentate NO^{2-}) are observed, indicating more final products were formed. In the range of 1260-860 cm^{-1}, although the tendency of adsorption bands is similar to that of CN (Table S4), one notable difference is that an obvious band associated with NO^+ appeared at 2175 cm^{-1} (Fig. S5d) under visible light irradiation.[2, 5, 8, 12, 13] Hadjiivanov et al. found that when NO was adsorbed onto surfaces possessing strong oxidative ability, an important reaction intermediate of NO oxidation—NO^+ was usually observed.[13] The adsorbed NO^+ tend to be preferentially oxidized to nitro compounds by reactive oxygen species in comparison with other nitrogen-containing species.[15, 16] Furthermore, the intensity of absorption bands at 866, 1001 cm^{-1} (Fig. S5d) was increased progressively but adsorption bands of N_2O disappeared, which indicates that NO on the surface of CN-C2 is gradually transformed to the final products. These final products accumulated on the photocatalyst surface can be removed easily by water washing.

Tables:

Table S1 The SBET, pore volume, Band gap value, NO removal ratio of CN, CN-C1, CN-C2, CN-C3.

Sample	S_{BET} (m^2g^{-1})	Pore volume (cm^3g^{-1})	Band gap (eV)	NO η(%)
CN	81	0.42	2.71	33.23
CN-C1	89	0.42	2.67	50.89
CN-C2	118	0.61	2.65	56.77
CN-C3	118	0.65	2.63	53

Table S2 Assignments of the IR bands observed during NO adsorption over CN

Wavenumbers (cm^{-1})	Assignment	References
888	NO_2^-	6
1009	nitrates	4
1081	Bidentate nitrates or monodentate nitrites	5,7,8
1133	NOH/NO^-	3
1148	NOH/NO^-	3
1163	NOH/NO^-	3
2136	N_2O	1,2

Table S3 Assignments of the IR bands observed during NO adsorption over CN-C2

Wavenumbers (cm^{-1})	Assignment	References
864	Chelated nitrite	11
881	NO_2^-	6
910	N_2O_4	6
985	Chelating bidentate NO_3^- species	17
1001	Bridging nitrates	4
1025	NO	18
1081	Bidentate nitrates or monodentate nitrites	5,7,8
1106	Nitrites	4
1122	Bidentate NO_2^-	4,2
1142	NOH/NO^-	3
1158	NOH/NO^-	3
2095	NO_2	4
2136	N_2O	1,2

Table S4 Assignments of the IR bands observed during photocatalytic NO oxidation over CN

Wavenumbers (cm^{-1})	Assignment	References
864	Chelated nitrite	11
883	NO_2^-	6
1009	Nitrates	4
1081	Bidentate nitrates or monodentate nitrites	5,7,8
1133	NOH/NO^-	3
1148	NOH/NO^-	3
1163	NOH/NO^-	3

Table S5 Assignments of the IR bands observed during photocatalytic NO oxidation over CN-C2

Wavenumbers (cm^{-1})	Assignment	References
866	Chelated nitrite	11
881	NO_2^-	6
910	N_2O_4	6
984	Chelated bidentate NO_3^- species	17
1001	Bridging nitrates	4
1042	Nitrates	4,5,7
1084	Bidentate nitrates or monodentate nitrites	5,7,8
1106	Nitrites	4
1143	NOH/NO^-	3
1160	NOH/NO^-	3
2095	NO_2	4
2175	NO^+	2,5,8,12,13

REFERENCES

1. R. Asahi, T. Morikawa, T. Ohwaki, K. Aoki and Y. Taga, Science, 2001, 293, 269-271.
2. J. Zhu, P. Xiao, H. Li and S. A. C. Carabineiro, ACS Appl. Mater. Interfaces, 2014, 6, 16449-16465.
3. K. Hadjiivanov, V. Avreyska, D. Klissurski and T. Marinova, Langmuir, 2002, 18, 1619-1625.
4. X. C. Wang, K. Maeda, A. Thomas, K. Takanabe, G. Xin, J. M. Carlsson, K. Domen and M. Antonietti, Nature, 2008, 271-275.
5. G. Liu, P. Niu, C. Sun, S. C. Smith, Z. Chen, G. Lu and H. Cheng, J. Am. Chem. Soc., 2010, 132, 11642-11648.
6. Y. Bi, S. X. Ouyang, N. Umezawa, J. Cao and J. Ye, J. Am. Chem. Soc., 2011, 133, 6490-6492.
7. S. Sun and W. Wang, RSC Adv., 2014, 4, 47136-47152.
8. J. Zhang, B. Wang and X. Wang, Prog. Chem., 2014, 26, 19-29.
9. Y. Lin and D. Su, ACS Nano., 2014, 8, 7823-33.
10. J. Li, J. Liu, S. Yin, Y. Liu, J. Li, W. Cen and Y. Chu, RSC Adv., 2016, 86316-86323.
11. G. Dong, Y. Zhang, Q. Pan and J. Qiu, J. Photoch. Photobi. C., 2014, 20, 33-50.
12. Y. Tian, B. Chang, Z. Yang, B. Zhou, F. Xi and X. Dong, RSC Adv., 2013, 4, 4187-4193.
13. Y. Bu and Z. Chen, RSC Adv., 2014, 4, 45397-45406.
14. K. Hadjiivanov, Cat. Rev. Sci. Eng., 2000, 42, 71-144.
15. L. Zhong, Y. Yu, W. Cai, X. Geng and Q. Zhong, Phys. Chem. Chem. Phys., 2015,17, 15036-15045.
16. N. Tang, Y. Liu, H. Wang and Z. Wu, J. Phys. Chem. C, 2011, 115, 8214-8220.
17. X. Li, X. Wang and M. Antonietti, ACS Catal., 2012, 2, 2082–2086.
18. M. Schraml-Marth, A. Wokaun, H. E. Curry-Hyde and A. Baiker, J. Catal., 1992, 133, 431-444.